Rotation of fullerene molecules in the crystal lattice of fullerene/porphyrin: C_{60} and $Sc_3N@C_{80}$

Yajuan Hao, Yaofeng Wang, Lukas Spree, and Fupin Liu

Electronic Supplementary Information

Contents

1. Crystal data

Table S1. Crystal data_$Sc_3N@C_{80}$.

Crystal	$Sc_3N@C_{80}$□NiOEP□2(C_6H_6)	$Sc_3N@C_{80}$□NiOEP□2(C_6H_6)	$Sc_3N@C_{80}$□NiOEP□2(C_6H_6)
Formula	$C_{128}H_{56}N_5NiSc_3$	$C_{128}H_{56}N_5NiSc_3$	$C_{128}H_{56}N_5NiSc_3$
Formula weight	1857.36	1857.36	1857.36
Color, habit	Black, block	Black, block	Black, block
Crystal system	triclinic	triclinic	triclinic
Space group	$P\bar{1}$	$P\bar{1}$	$P\bar{1}$
***a*, Å**	14.720(3)	14.740(3)	14.750(3)
***b*, Å**	15.390(3)	15.410(3)	15.440(3)
***c*, Å**	17.670(4)	17.700(4)	17.730(4)
***α*, deg**	81.17(3)	81.20(3)	81.22(3)
***β*, deg**	74.54(3)	74.54(3)	74.56(3)
***γ*, deg**	86.24(3)	86.28(3)	86.31(3)
Volume, Å³	3811.1(15)	3828.1(15)	3845.3(15)
Z	2	2	2
***T*, K**	100	130	160
Radiation (λ, Å)	Synchrotron Radiation (0.7999)	Synchrotron Radiation (0.7999)	Synchrotron Radiation (0.7999)
Unique data (R_{int})	20749 (0.0289)	20850 (0.0407)	20938 (0.0559)
Parameters	1333	1353	1363
Restraints	133	175	240
Observed data (*I* > 2*σ*(*I*))	20586	20656	20585
R_1^a (observed data)	0.0875	0.0922	0.0983
wR_2^b (all data)	0.2417	0.2615	0.2841
CCDC NO.	2027144	2027145	2027146

[a]For data with $I > 2\sigma(I)$, $R_1 = \frac{\sum||F_o| - |F_c||}{\sum|F_o|}$. [b]For all data, $wR_2 = \sqrt{\frac{\sum\left[w\left(F_o^2 - F_c^2\right)^2\right]}{\sum\left[w\left(F_o^2\right)^2\right]}}$.

Table S1. Crystal data_$Sc_3N@C_{80}$_continued.

Crystal	$Sc_3N@C_{80}$□NiOEP□2(C_6H_6)	$Sc_3N@C_{80}$□NiOEP□2(C_6H_6)	$Sc_3N@C_{80}$□NiOEP□2(C_6H_6)
Formula	$C_{128}H_{56}N_5NiSc_3$	$C_{128}H_{56}N_5NiSc_3$	$C_{128}H_{56}N_5NiSc_3$
Formula weight	1857.36	1857.36	1857.36
Color, habit	Black, block	Black, block	Black, block
Crystal system	triclinic	triclinic	triclinic
Space group	$P\bar{1}$	$P\bar{1}$	$P\bar{1}$
***a*, Å**	14.770(3)	14.790(3)	14.810(3)
***b*, Å**	15.460(3)	15.480(3)	15.490(3)
***c*, Å**	17.770(4)	17.820(4)	17.880(4)
***α*, deg**	81.21(3)	81.16(3)	81.12(3)
***β*, deg**	74.99(3)	74.31(3)	74.16(3)
***γ*, deg**	86.28(3)	86.17(3)	86.10(3)
Volume, Å³	3871.8(15)	3879.8(15)	3897.3(15)
Z	2	2	2
***T*, K**	190	220	250
Radiation (λ, Å)	Synchrotron Radiation (0.7999)	Synchrotron Radiation (0.7999)	Synchrotron Radiation (0.7999)
Unique data (R_{int})	21056 (0.0447)	21197 (0.0475)	21172 (0.0217)
Parameters	1413	1433	1453
Restraints	1134	1362	1625
Observed data ($I > 2\sigma(I)$)	20690	20521	20467
R_1[a] (observed data)	0.0957	0.0988	0.1019
wR_2[b] (all data)	0.2893	0.3019	0.3140
CCDC NO.	2027147	2027148	2027149

[a]For data with $I > 2\sigma(I)$, $R_1 = \frac{\sum||F_o| - |F_c||}{\sum|F_o|}$. [b]For all data, $wR_2 = \sqrt{\frac{\sum\left[w\left(F_o^2 - F_c^2\right)^2\right]}{\sum\left[w\left(F_o^2\right)^2\right]}}$.

Table S1. Crystal data_$Sc_3N@C_{80}$_continued.

Crystal	$Sc_3N@C_{80}$□NiOEP□2(C_6H_6)
Formula	$C_{128}H_{56}N_5NiSc_3$
Formula weight	1857.36
Color, habit	Black, block
Crystal system	triclinic
Space group	$P\bar{1}$
***a*, Å**	14.830(3)
***b*, Å**	15.500(3)
***c*, Å**	17.930(4)
***α*, deg**	81.08(3)
***β*, deg**	74.03(3)
***γ*, deg**	86.05(3)
Volume, Å³	3913.0(15)
Z	2
***T*, K**	280
Radiation (λ, Å)	Synchrotron Radiation (0.7999)
Unique data (R_{int})	21315 (0.0234)
Parameters	1451
Restraints	1655
Observed data ($I > 2\sigma(I)$)	20430
R_1[a] (observed data)	0.1060
wR_2[b] (all data)	0.3292
CCDC NO.	2027150

[a]For data with $I > 2\sigma(I)$, $R_1 = \frac{\sum||F_o| - |F_c||}{\sum|F_o|}$. [b]For all data, $wR_2 = \sqrt{\frac{\sum\left[w\left(F_o^2 - F_c^2\right)^2\right]}{\sum\left[w\left(F_o^2\right)^2\right]}}$.

Table S2. Crystal data_C_{60}.

Crystal	C_{60}⊃NiOEP⊃2(C_6H_6)	C_{60}⊃NiOEP⊃2(C_6H_6)	C_{60}⊃NiOEP⊃2(C_6H_6)
Formula	$C_{108}H_{56}N_4Ni$	$C_{108}H_{56}N_4Ni$	$C_{108}H_{56}N_4Ni$
Formula weight	1468.27	1468.27	1468.27
Color, habit	Black, block	Black, block	Black, block
Crystal system	triclinic	triclinic	triclinic
Space group	$P\bar{1}$	$P\bar{1}$	$P\bar{1}$
***a*, Å**	14.130(3)	14.130(3)	14.130(3)
***b*, Å**	14.380(3)	14.410(3)	14.440(3)
***c*, Å**	17.200(3)	17.290(4)	17.410(4)
***α*, deg**	87.54(3)	87.72(3)	87.96(3)
***β*, deg**	75.78(3)	75.78(3)	75.78(3)
***γ*, deg**	75.61(3)	75.74(3)	75.92(3)
Volume, Å^3	3280.9(13)	3306.7(13)	3338.9(13)
Z	2	2	2
***T*, K**	100	160	220
Radiation (λ, Å)	Synchrotron Radiation (0.7999)	Synchrotron Radiation (0.7999)	Synchrotron Radiation (0.7999)
Unique data (R_{int})	17754 (0.0225)	17893 (0.0506)	18160 (0.0363)
Parameters	1026	1026	1027
Restraints	0	0	0
Observed data ($I > 2\sigma(I)$)	17546	17811	18041
R_1^a (observed data)	0.0383	0.0486	0.0589
wR_2^b (all data)	0.1015	0.1308	0.1679
CCDC NO.	2027151	2027152	2027153

[a]For data with $I > 2\sigma(I)$, $R_1 = \frac{\sum ||F_o| - |F_c||}{\sum |F_o|}$. [b]For all data, $wR_2 = \sqrt{\frac{\sum \left[w\left(F_o^2 - F_c^2\right)^2\right]}{\sum \left[w\left(F_o^2\right)^2\right]}}$.

Table S2. Crystal data_C_{60}_continued.

Crystal	C_{60}⊇NiOEP⊇2(C_6H_6)
Formula	$C_{108}H_{56}N_4Ni$
Formula weight	1468.27
Color, habit	Black, block
Crystal system	triclinic
Space group	$P\bar{1}$
***a*, Å**	14.150(3)
***b*, Å**	14.470(3)
***c*, Å**	17.520(4)
***α*, deg**	88.18(3)
***β*, deg**	75.80(3)
***γ*, deg**	76.08(3)
Volume, Å^3	3374.1(13)
Z	2
***T*, K**	280
Radiation (λ, Å)	Synchrotron Radiation (0.7999)
Unique data (R_{int})	18384 (0.0500)
Parameters	1015
Restraints	24
Observed data ($I > 2\sigma(I)$)	18188
R_1[a] (observed data)	0.0688
wR_2[b] (all data)	0.2005
CCDC NO.	2027154

[a]For data with $I > 2\sigma(I)$, $R_1 = \frac{\sum||F_o| - |F_c||}{\sum|F_o|}$. [b]For all data, $wR_2 = \sqrt{\frac{\sum\left[w\left(F_o^2 - F_c^2\right)^2\right]}{\sum\left[w\left(F_o^2\right)^2\right]}}$.

2. Structure parameters

Table S3. Nearest cage carbon-Ni contact distances as a function of temperature

Temperature (K)	100	130	160	190	220	250	280
$Ho_2LuN@C_{80}$ (Å)[1]	2.810(6)	2.812(7)	2.795(8)	2.81(1)	-	2.85(2)	2.86(2)
$Lu_3N@C_{80}$ (Å)[1]	2.79(2)	-	2.83(1)	-	2.83(3)	-	2.83(2)
$Sc_3N@C_{80}$ (Å)	2.766(3)	2.774(4)	2.787(4)	2.809(4)	2.821(5)	2.835(6)	2.846(6)
C_{60} (Å)	3.006(2)	-	3.025(2)	-	3.054(3)	-	3.089(4)

Table S4. Metal site occupancy in $Sc_3N@C_{80}$ as a function of temperatures

Temperature (K)	100	130	160	190	220	250	280
Sc1	0.231(3)	0.246(3)	0.276(3)	0.223(6)	0.213(5)	0.199(5)	0.190(5)
Sc2	0.478(3)	0.395(3)	0.334(3)	0.206(6)	0.179(6)	0.168(6)	0.152(6)
Sc3	0.290(3)	0.239(3)	0.198(3)	0.120(5)	0.105(5)	0.096(5)	0.086(5)
Sc4	0.183(3)	0.175(3)	0.107(3)	0.081(4)	0.084(4)	0.089(4)	0.101(4)
Sc5	0.202(3)	0.197(3)	0.108(3)	0.076(4)	0.076(4)	0.081(4)	0.083(4)
Sc6	0.170(3)	0.196(3)	0.197(3)	0.150(5)	0.141(5)	0.154(7)	0.149(7)
Sc7	0.213(3)	0.205(3)	0.198(3)	0.132(4)	0.132(5)	0.126(5)	0.117(5)
Sc8	0.225(3)	0.226(3)	0.219(3)	0.102(5)	0.090(4)	0.069(4)	0.070(4)
Sc9	0.464(3)	0.378(3)	0.352(3)	0.235(7)	0.220(6)	0.200(6)	0.184(5)
Sc10	0.136(3)	0.153(3)	0.154(3)	0.148(5)	0.168(6)	0.078(6)	0.095(6)
Sc11	0.070(3)	0.095(3)	0.231(3)	0.110(5)	0.109(5)	0.089(5)	0.085(5)
Sc12	0.232(3)	0.233(3)	0.222(3)	0.164(5)	0.158(5)	0.157(5)	0.144(5)
Sc13	0.107(3)	0.107(3)	0.133(3)	0.126(6)	0.099(5)	0.095(5)	0.090(4)
Sc14		0.080(3)	0.102(3)	0.076(4)	0.101(5)	0.108(5)	0.110(5)
Sc15		0.075(3)	0.102(3)	0.070(3)	0.083(4)	0.099(4)	0.094(4)
Sc16			0.068(3)	0.055(4)	0.079(4)	0.087(5)	0.102(5)
Sc17				0.052(3)	0.081(4)	0.088(4)	0.091(4)
Sc18				0.074(3)	0.087(4)	0.091(4)	0.100(4)
Sc19				0.093(5)	0.104(5)	0.073(5)	0.080(5)
Sc20				0.101(5)	0.100(5)	0.106(5)	0.094(5)
Sc21				0.080(5)	0.083(5)	0.082(4)	0.081(4)
Sc22					0.049(4)	0.048(4)	0.058(4)
Sc23					0.053(4)	0.119(5)	0.114(5)
Sc24						0.117(5)	0.120(6)
Sc25						0.051(4)	0.047(4)
Sc26							0.051(4)

3. Ellipsoids comparison on variable temperatures

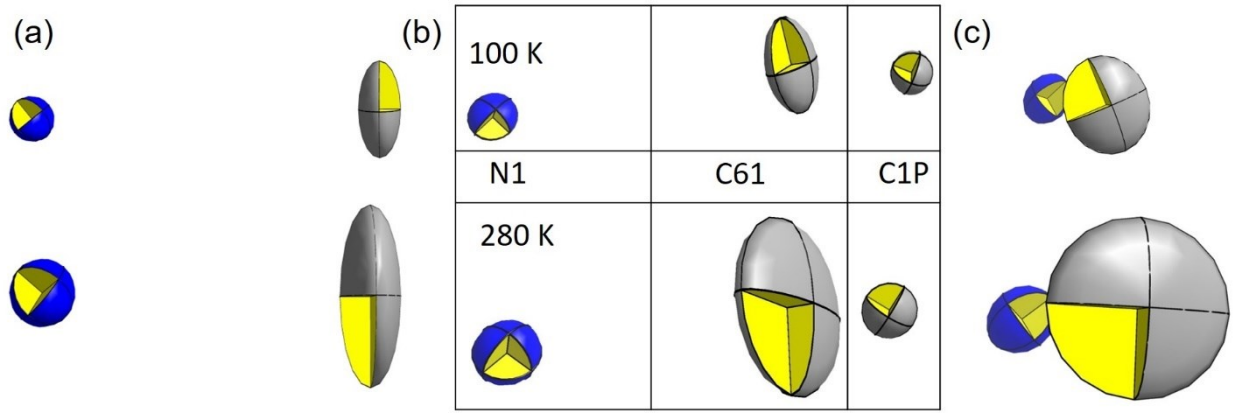

Figure S1. Ellipsoids of C1P of NiOEP and C61 of C80 fullerene cage at 100 and 280 K highlighted at 80% probability level. The N1 of the Sc_3N cluster is drawn to show the orientation of the C61 as well as its ellipsoid changes on temperature. (a) shows the ellipsoids viewed from the lateral direction of C61 to highlight the increment of the radial direction; (b) is shown in Figure 1 in the manuscript to view both the radial and lateral directions properly; (c) shows the ellipsoids viewed from the radial direction of C61 to highlight the increment of the lateral direction.

4. Reported pristine $Sc_3N@C_{80}$ structure

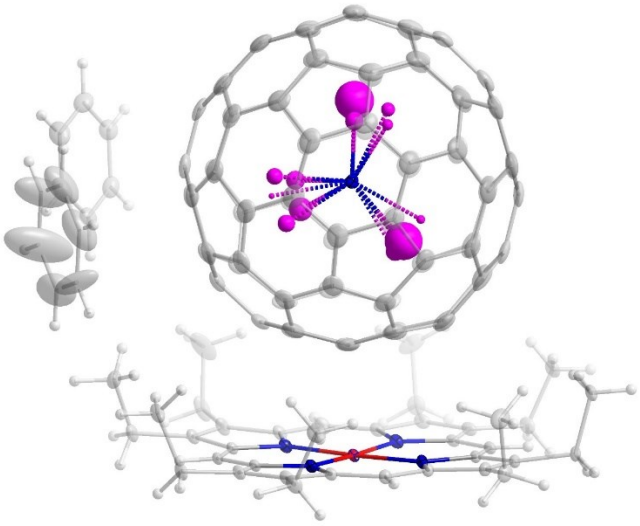

Figure S2. $Sc_3N@C_{80}$/NiOEP/benzene, 100K. The metal sites are shown as spheres whose radii are scaling proportional to the site occupancy (the bigger the sphere, the higher the occupancy). The displacement parameters are shown at the 30% probability level. Color code: grey for carbon, blue for nitrogen, white for hydrogen, red for nickel, and pink for scandium.

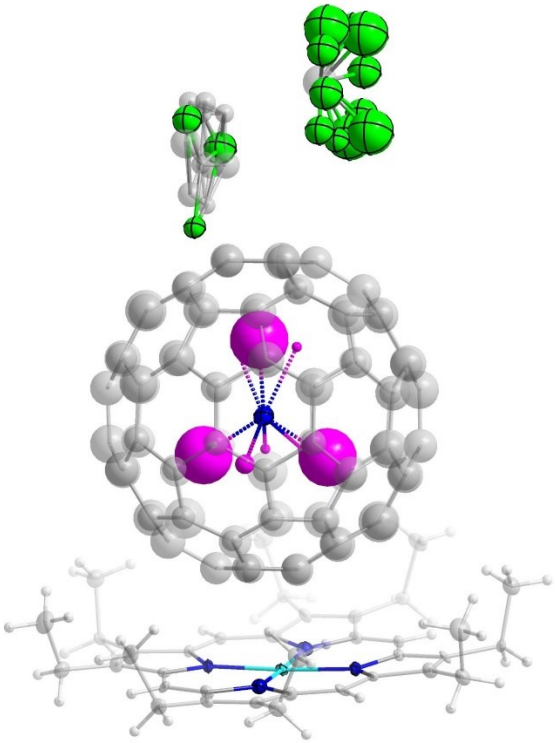

Figure S3. $Sc_3N@C_{80}$/CoOEP/benzene/chloroform, 130K. Drawn with the data from ref. [2] The metal sites are shown as spheres whose radii are scaling proportional to the site occupancy (the bigger the sphere, the higher the occupancy). The displacement parameters are shown at the 30% probability level. Color

code: grey for carbon, blue for nitrogen, green for chlorine, white for hydrogen, cyan for cobalt, and pink for scandium.

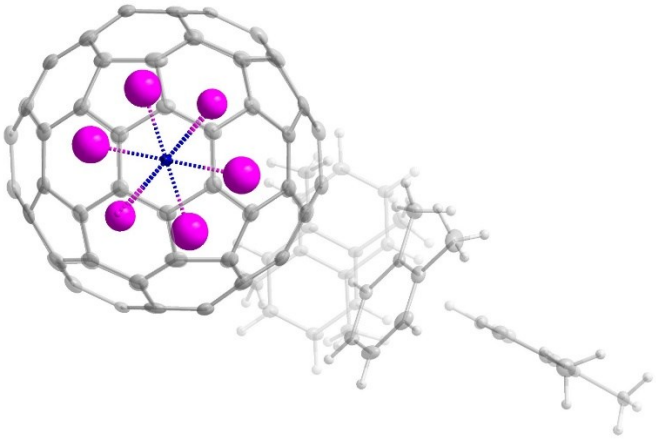

Figure S4. $Sc_3N@C_{80}$/*o*-xylene, 90K. Drawn with the data from ref. [3] The metal sites are shown as spheres whose radii are scaling proportional to the site occupancy (the bigger the sphere, the higher the occupancy). The displacement parameters are shown at the 30% probability level. Color code: grey for carbon, blue for nitrogen, white for hydrogen, and pink for scandium.

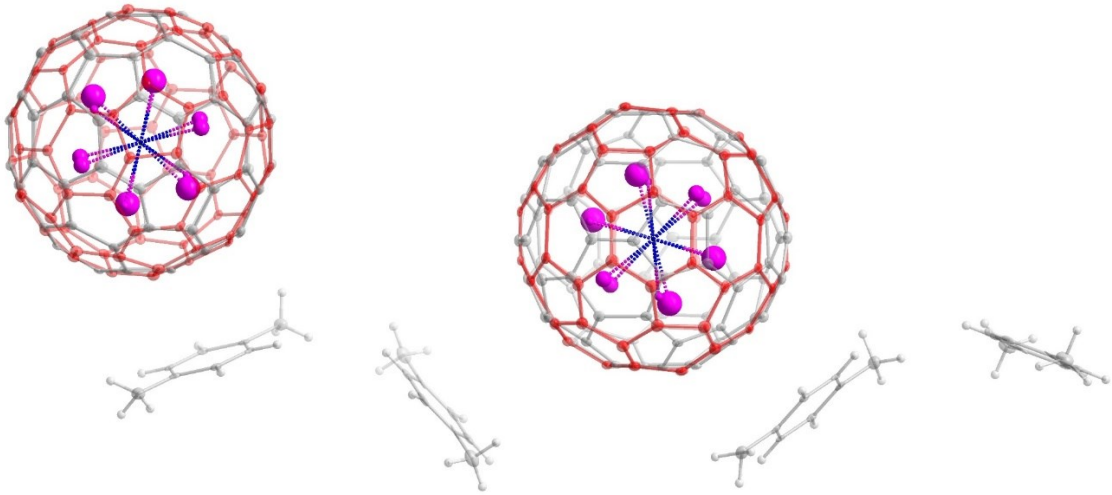

Figure S5. $Sc_3N@C_{80}$/*p*-xylene, two orientations of the C_{80} cage, 100K. Drawn with the data from ref. [4] The metal sites are shown as spheres whose radii are scaling proportional to the site occupancy (the bigger the sphere, the higher the occupancy). The displacement parameters are shown at the 30% probability level. Color code: grey for carbon, blue for nitrogen, white for hydrogen, and pink for scandium. The two orientations of the fullerene cage are differentiated by colors (grey and red).

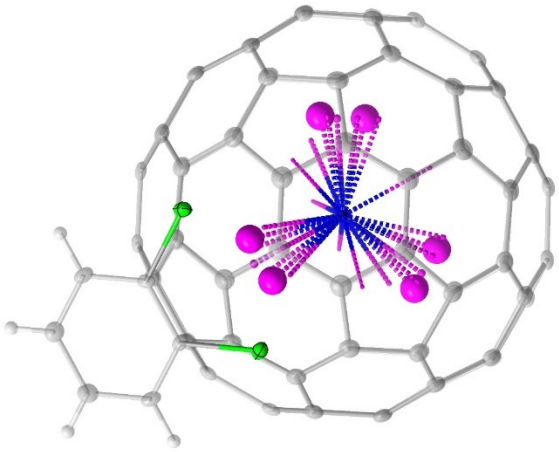

Figure S6. $Sc_3N@C_{80}$/*o*-DCB, 100K. Drawn with the data from ref. [5] The metal sites are shown as spheres whose radii are scaling proportional to the site occupancy (the bigger the sphere, the higher the occupancy). The displacement parameters are shown at the 30% probability level. Color code: grey for carbon, blue for nitrogen, white for hydrogen, green for chlorine, and pink for scandium.

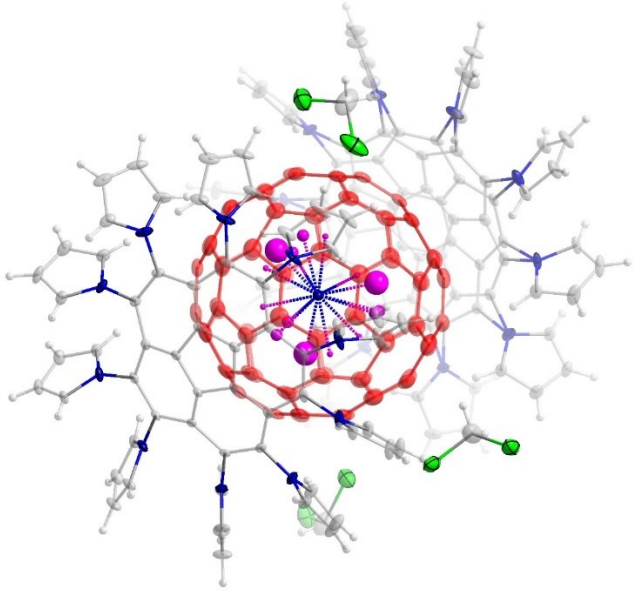

Figure S7. $Sc_3N@C_{80}$/decapyrrylcorannulene/dichloromethane, 100K. Drawn with the data from ref. [6] The metal sites are shown as spheres whose radii are scaling proportional to the site occupancy (the bigger the sphere, the higher the occupancy). The displacement parameters are shown at the 30% probability level. Color code: grey for carbon, blue for nitrogen, white for hydrogen, green for chlorine, and pink for scandium. The fullerene cage is highlighted with red color from the co-crystallized decapyrrylcorannulene.

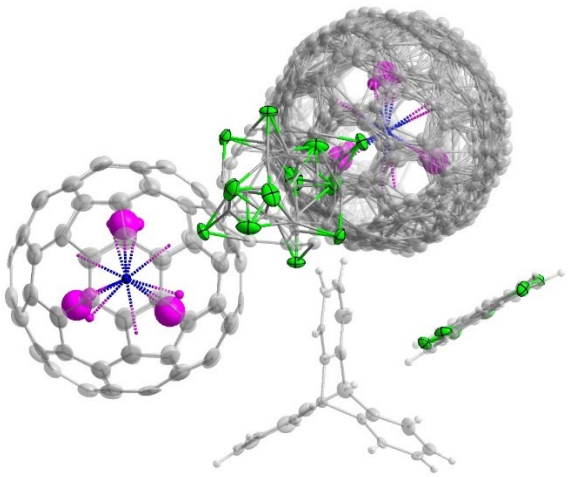

Figure S8. $Sc_3N@C_{80}$/triptycene/*o*-DCB, 100K. Drawn with the data from ref. [5] The metal sites are shown as spheres whose radii are scaling proportional to the site occupancy (the bigger the sphere, the higher the occupancy). The displacement parameters are shown at the 30% probability level. Color code: grey for carbon, blue for nitrogen, white for hydrogen, green for chlorine, and pink for scandium.

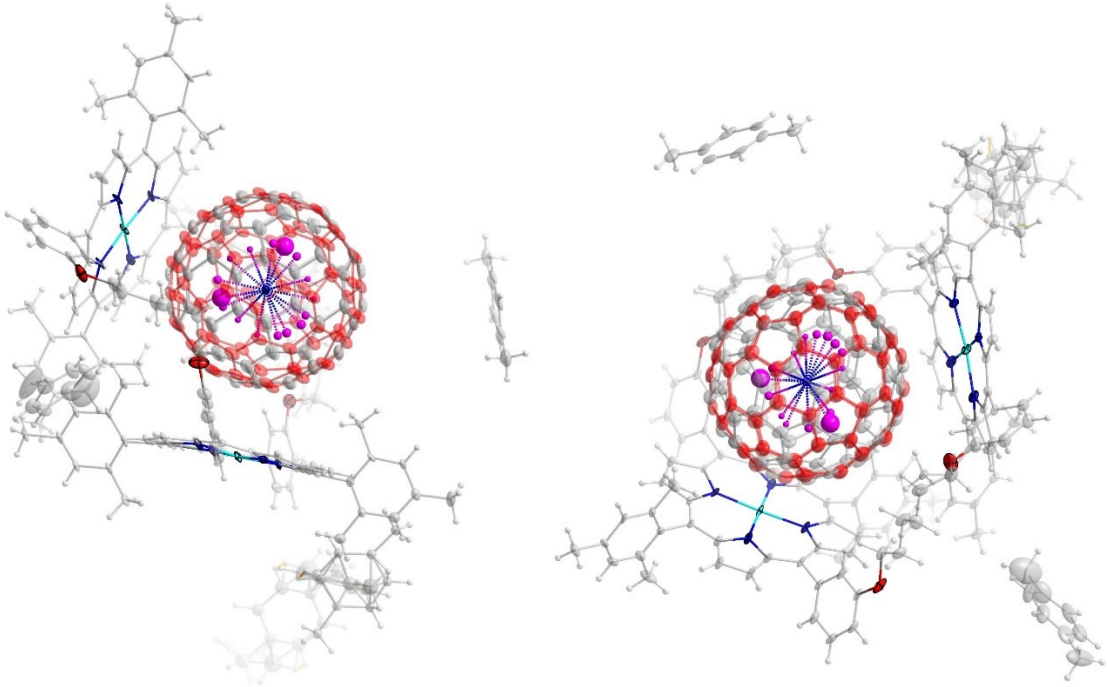

Figure S9. $Sc_3N@C_{80}$/Zn_2BisPy/*p*-xylene-1, two orientations of the C_{80} cage, 100K. Drawn with the data from ref. [4] The metal sites are shown as spheres whose radii are scaling proportional to the site occupancy (the bigger the sphere, the higher the occupancy). The displacement parameters are shown at the 30% probability level. Color code: grey for carbon, blue for nitrogen, white for hydrogen, red for oxygen, cyan for zinc, and pink for scandium. The two orientations of the fullerene cage are differentiated by colors (grey and red).

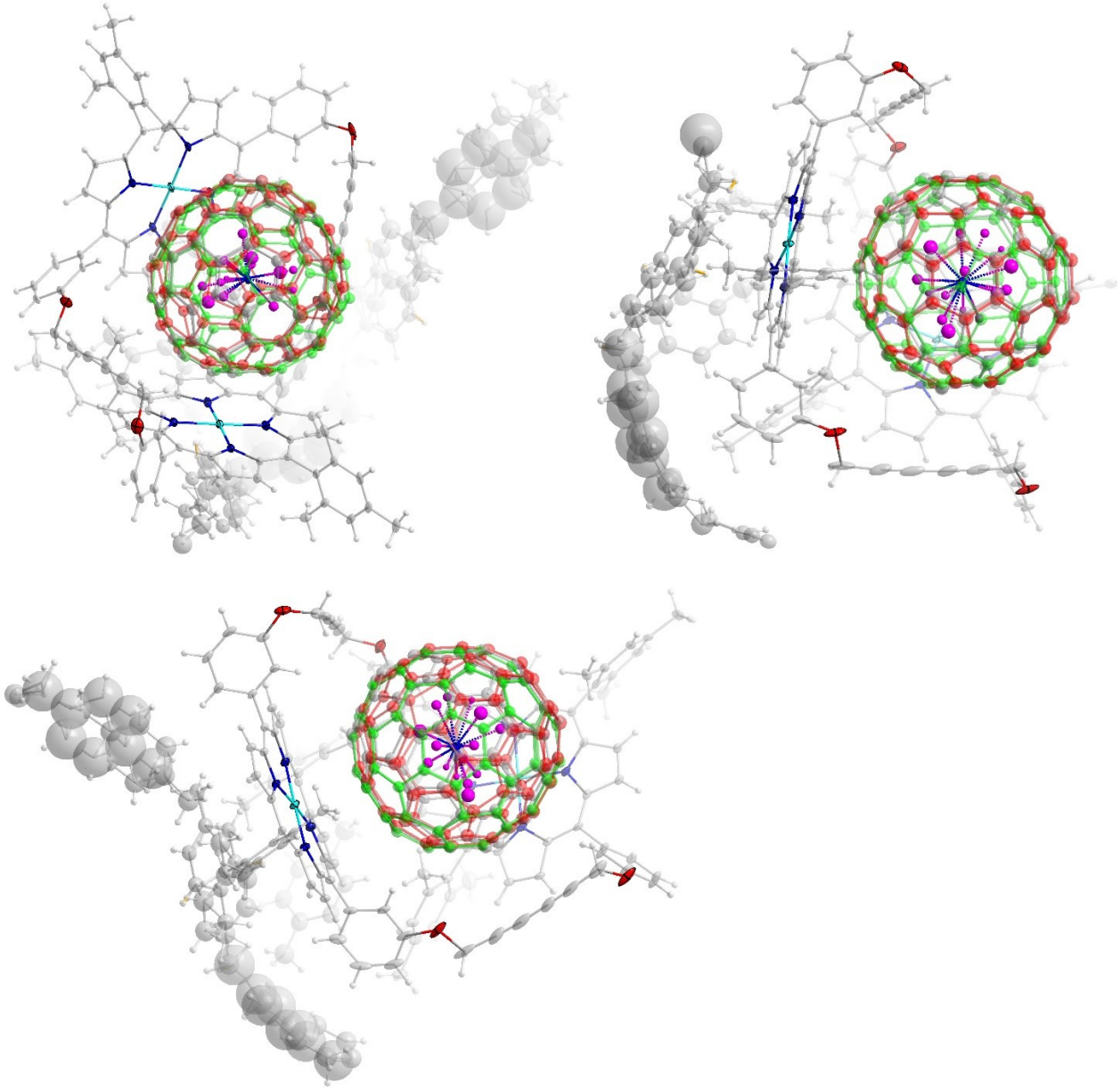

Figure S10. $Sc_3N@C_{80}/Zn_2BisPy/p$-xylene-2, three orientations of the C_{80} cage, 100K. Drawn with the data from ref. [4] The metal sites are shown as spheres whose radii are scaling proportional to the site occupancy (the bigger the sphere, the higher the occupancy). The displacement parameters are shown at the 30% probability level. Color code: grey for carbon, blue for nitrogen, white for hydrogen, red for oxygen, cyan for zinc, and pink for scandium. The three orientations of the fullerene cage are differentiated by colors (grey, red, and green).

5. Temperature driven dynamics of Sc_3N and Ho_2LuN clusters in C_{80}.

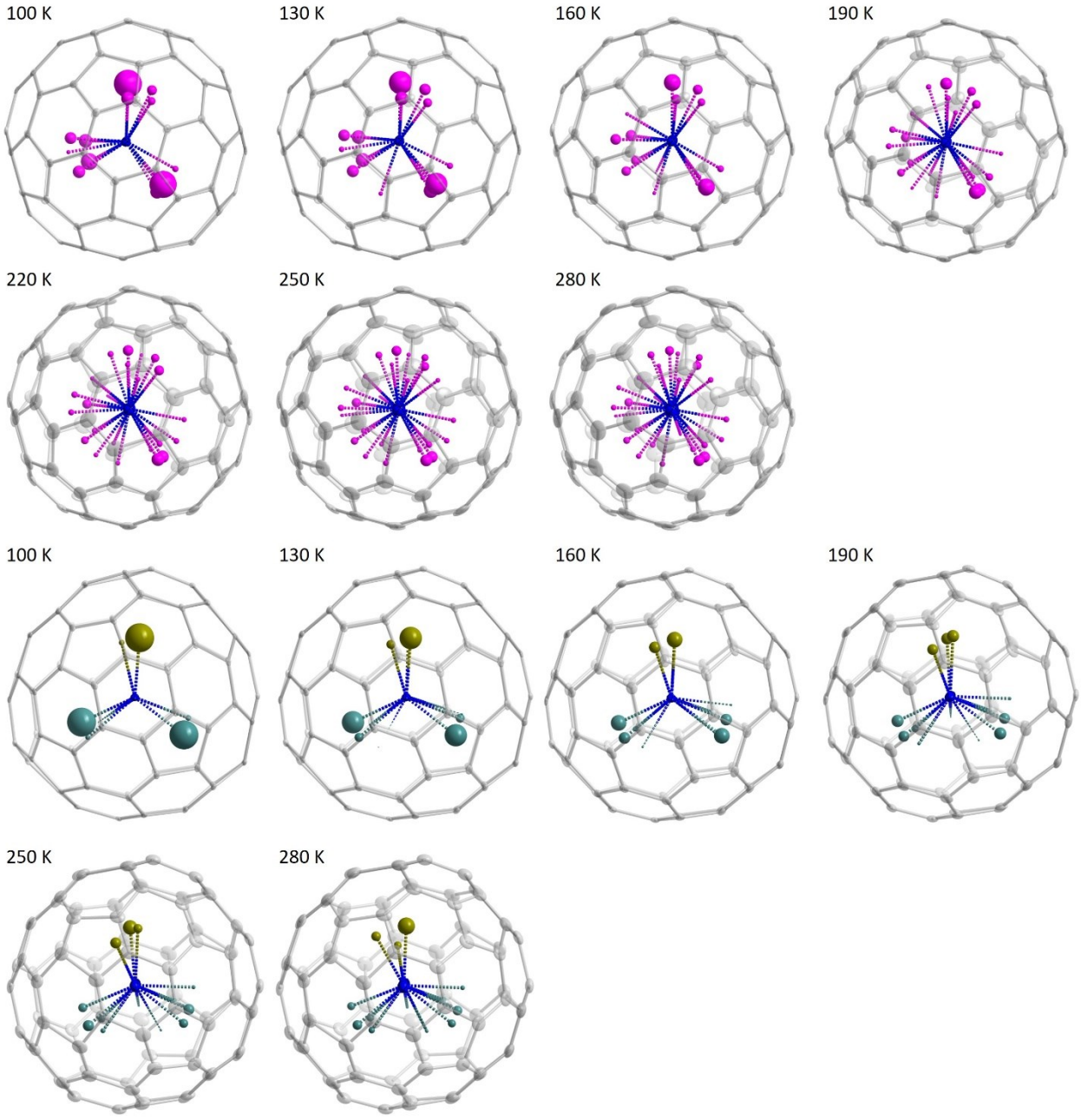

Figure S11. Molecular structure of $Sc_3N@C_{80}$·NiOEP·2(C_6H_6) measured with single-crystal X-ray diffraction at variable temperatures from 100 to 280 K. The metal sites are shown as spheres whose radii are scaling proportional to the site occupancy (the bigger the sphere, the higher the occupancy). Color code: grey for carbon, pink for Sc, and blue for N. As comparison, the molecular structure of $Ho_2LuN@C_{80}$·NiOEP·2(C_6H_6) measured with single-crystal X-ray diffraction at variable temperatures from 100 to 280 K was shown.[9] The metal sites are shown as spheres whose radii are scaling proportional to the site occupancy (the bigger the sphere, the higher the occupancy). Color code: grey for carbon, brown for Lu, cyan for Ho, and blue for N.

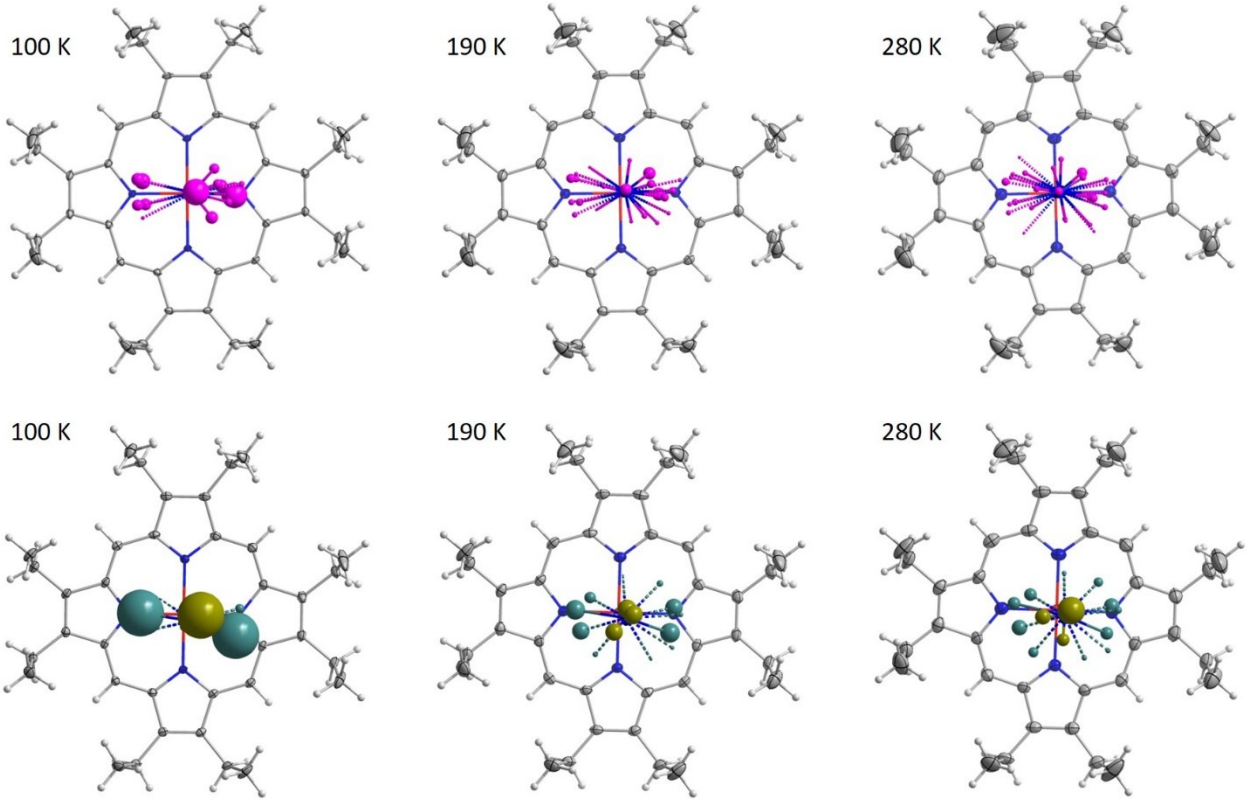

Figure S12. Molecular structures of $Sc_3N@C_{80}$/NiOEP and $Ho_2LuN@C_{80}$/NiOEP measured at variable temperatures. To highlight the relative position of the M_3N cluster to the NiOEP, C_{80} cage and the solvent molecules are omitted for clarity. The displacement parameters are shown at the 30% probability level except for the M_3. The M_3 sites are shown as spheres whose radii are scaling proportional to the site occupancy (the bigger the sphere, the higher the occupancy). Color code: grey for carbon, blue for nitrogen, white for hydrogen, red for nickel, pink for scandium, brown for Lu, and cyan for Ho.

6. References

1. F. Liu and L. Spree, Molecular Spinning Top: Visualizing the Dynamics of $M_3N@C_{80}$ with Variable Temperature Single Crystal X-ray Diffraction, *Chem. Commun.*, 2019, **55**, 13000-13003.
2. S. Stevenson, G. Rice, T. Glass, K. Harich, F. Cromer, M. R. Jordan, J. Craft, E. Hadju, R. Bible, M. M. Olmstead, K. Maitra, A. J. Fisher, A. L. Balch and H. C. Dorn, Small-bandgap endohedral metallofullerenes in high yield and purity, *Nature*, 1999, **401**, 55-57.
3. S. Stevenson, H. M. Lee, M. M. Olmstead, C. Kozikowski, P. Stevenson and A. L. Balch, Preparation and crystallographic characterization of a new endohedral, $Lu_3N@C_{80}$·5 (*o*-xylene), and comparison with $Sc_3N@C_{80}$·5 (*o*-xylene), *Chem. Eur. J.*, 2002, **8**, 4528-4535.
4. L. P. Hernández-Eguía, E. C. Escudero-Adán, J. R. Pinzón, L. Echegoyen and P. Ballester, Complexation of $Sc_3N@C_{80}$ Endohedral Fullerene with Cyclic Zn-Bisporphyrins: Solid State and Solution Studies, *J. Org. Chem.*, 2011, **76**, 3258-3265.
5. D. Konarev, A. A. Popov, L. V. Zorina, S. S. K. Khasanov and R. N. Lyubovskaya, Molecular structure, magnetic and optical properties of endometallonitridofullerene $Sc_3N@I_h$-C_{80} in neutral, radical anion and dimeric anionic forms, *Chem. Eur. J.*, 2019, **25**, 14858-14869.

6. Y.-Y. Xu, H.-R. Tian, S.-H. Li, Z.-C. Chen, Y.-R. Yao, S.-S. Wang, X. Zhang, Z.-Z. Zhu, S.-L. Deng, Q. Zhang, S. Yang, S.-Y. Xie, R.-B. Huang and L.-S. Zheng, Flexible decapyrrylcorannulene hosts, *Nat. Commun.*, 2019, **10**, 485.